AIAA JOURNAL
Vol. 43, No. 1, January 2005

Far-Field Acoustic Investigation into Chevron Nozzle Mechanisms and Trends

B. Callender* and E. Gutmark†
University of Cincinnati, Cincinnati, Ohio 45221
and
S. Martens‡
General Electric Aircraft Engines, Cincinnati, Ohio 45215

Chevron nozzles currently offer one of the most feasible methods of reducing jet exhaust noise in medium to high-bypass turbofan engines. Tests were conducted in the University of Cincinnati Nozzle Acoustic Test Facility, simulating a separate flow exhaust system to provide insight into some of the basic mechanisms and trends of this emerging technology. For this study, a baseline inner nozzle and three chevron nozzles were tested over a wide range of operating conditions, including dual and single flow. Chevrons with varying numbers of lobes and levels of penetration were selected for this study to provide insight into the impact of these geometric parameters on the noise level. Spectral and directivity results from heated, coaxial flow tests showed that the chevron nozzles are most effective at lower frequencies and at aft directivity angles. Reductions in overall sound pressure level (SPL) ranging from 3 to 6 dB were documented. Calculations of perceived noise level directivity also showed 4–6 dB reduction at aft angles. The data also illustrated clear and consistent trends with respect to the chevron geometric parameters. Specifically, the chevron penetration was determined to be a primary factor in controlling the tradeoff between low-frequency reduction and high-frequency SPL increases. Although slight differences were observed with varying chevron lobe numbers at a fixed penetration, it appears that the effect is less significant than the penetration. Finally, the data indicated clear dependence of the chevron benefit on the velocity difference between the inner and outer streams.

Introduction

SINCE the introduction of the high-bypass turbofan engine in the early to mid-1970s, there have been few significant advances in practical jet-noise-reduction techniques. However, a great deal of effort has been dedicated to the development of practical passive flow control techniques for jet noise reduction. Two techniques that have been the subject of extensive research are tabbed nozzles and multilobed mixers. Tabs were first investigated by Bradbury et al. and found to dramatically modify the jet plume.[1]

Specifically, a substantial increase in the centerline velocity decay was seen, indicating a shortening of the jet potential core. Since this pioneering effort, many other researchers have explored the flow mechanisms and potential acoustic benefit of tabbed nozzles.[2–6]

Samimy exhibited that the individual tabs generate a trail of counter-rotating vortices that increase mixing in the nozzle shear layer. However, almost without exception this increased mixing, while reducing low-frequency noise, generates excessive high-frequency noise. This high-frequency increase often erases any potential acoustic benefit. In addition to this, tabbed nozzles almost always result in some thrust loss.[6] Multilobed mixers feature multiple tubes or chutes to divide the inner core jet into several individual smaller jets. This breakup of the main jet results in enhanced mixing of the high-velocity inner flow with the surrounding outer bypass stream and a reduction in the length of the jet plume. This enhanced mixing can lead to reduced jet noise.[7,8] A byproduct of this enhanced mixing is the generation of a significant amount of high-frequency noise. This requires a long duct, typically lined with acoustic treatment, to shield and attenuate this noise source. Although effective in reducing jet noise, these lobed mixers have two distinct drawbacks. First, the complex geometries can substantially complicate fabrication resulting in increased costs. Furthermore, these nozzles can adversely impact the aircraft system through increased weight and scrubbing drag.

Chevron nozzles represent the current state of the art in jet-noise-reduction technology for application in medium- and high-bypass turbofan engines. These nozzles feature triangular serrations in the nozzle trailing edge, which induce streamwise vorticity into the shear layer. As with tabbed nozzles, this vorticity leads to increased mixing and reduced jet plume length. However, the level of penetration of the individual chevrons is typically much less than that for tabbed nozzles, and the induced vorticity is therefore weaker. As opposed to other noise-reduction technologies discussed, such as tabbed nozzles or multilobed mixers, chevron nozzles are capable of effectively reducing engine exhaust noise while imposing minimal engine performance penalty and a very small weight impact.

As a result of being such an attractive solution to the problem of jet noise, much of the research and development work that has been done with chevrons has been conducted by private industry and therefore remains proprietary in nature. The results of an extensive study conducted at NASA Glenn Research Center were recently published, identifying a set of chevron nozzle configurations providing reductions in jet effective perceived noise level (EPNL) of 2–3 EPNdB with minimal loss of nozzle thrust.[9] However, at the present time, there have been few published works seeking to improve the understanding of the fundamental mechanisms responsible for the acoustic benefit of chevron nozzles. This work seeks to provide some insight in this area through a basic parametric study of nozzle far-field acoustics. Although it is well understood that chevron nozzles can reduce peak jet noise by producing more efficient mixing of the high-velocity inner jet with the lower-speed fan stream and shortening of the potential core, the level of influence of the various geometric parameters remains somewhat unclear. The

Presented as Paper 2003-1058 at the AIAA 41st Aerospace Sciences Meeting, Reno, NV, 6–9 January 2003; received 3 November 2003; accepted for publication 10 August 2004.

*Ph.D. Student, Department of Aerospace Engineering and Engineering Mechanics; currently Lead Engineer, General Electric Aircraft Engines, Cincinnati, OH 45215.

†Professor and Ohio Eminent Scholar, Department of Aerospace Engineering and Engineering Mechanics.

‡Senior Engineer.

parameters that were investigated are the number of lobes, or individual chevrons, and the level of penetration of the chevrons into the flow. These parameters were investigated over a variety of flow conditions ranging from single nozzle flow to separate flow over a representative range of velocity differences. Three chevron core nozzles, as well as a baseline circular nozzle, were used in this study to investigate the impact of the chevron design on the acoustic benefit provided.

Test Setup and Facility

Acoustic tests were conducted in the University of Cincinnati (UC) Nozzle Acoustic Test Facility. This facility features a coaxial flow test rig capable of accurately simulating engine operating conditions in terms of nozzle pressure ratio and velocity difference. The rig is equipped with a separate flow exhaust model with core and fan exit areas of 3.62 in.^{2} (23.35 cm^2) and 12.57 in.^{2} (81.10 cm^2), respectively. Figure 1 shows a photograph of the baseline separate flow exhaust system used for the current study, whereas Fig. 2 shows the overall test rig. The test rig was recently validated against data acquired in the acoustic test facility at General Electric Aircraft Engines (GEAE) in Cincinnati, Ohio. In this validation, baseline nozzle acoustic data was determined to closely agree with data acquired in GEAE's proven facility. The details of this validation as well as the test rig features and capabilities are available in Ref. 10.

Figure 3 shows a schematic of the acoustic test facility. The test rig is installed away from the center of the room to permit a wide coverage area for acoustic measurements. A constant distance polar microphone array is used for collection of far-field acoustic data. Centered on a $12\frac{1}{2}$-ft (3.81-m) radius, the microphone distance corresponds to approximately 35 equivalent jet diameters relative to the current separate flow exhaust model. The microphone array is capable of capturing data at jet directivity angles ranging from 60 to 150 deg, with the directivity angle being measured from the jet centerline such that the flow direction is defined as 180 deg. Acoustic data are collected using eight Bruël and Kjaer Model $4939\frac{1}{4}$-in. condenser microphones. The microphone data are acquired, as a binary time record, using a pair of synchronized National Instruments model 4452 dynamic signal acquisition boards. The data are then postprocessed to provide both narrowband and one-third octave band (TOB) spectral data using custom written LabView® codes. In addition to spectral data, accurate calculation of overall sound pressure level (OASPL) is facilitated by passing the captured time signal through a fourth-order Butterworth high-pass filter to remove frequencies below the anechoic cutoff limit of the chamber. For the OASPL data that will be presented in this work, a filter cutoff frequency of 500 Hz was utilized.

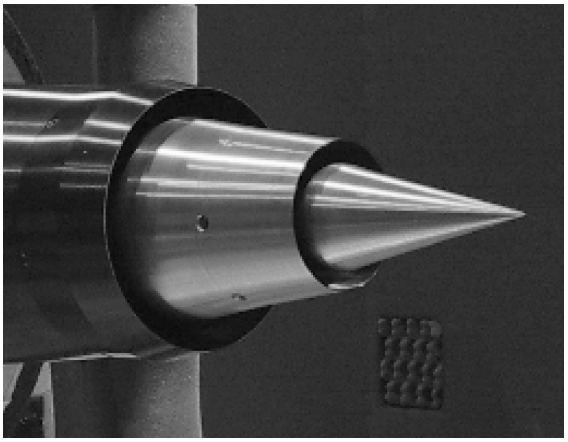

Fig. 1 Detail of separate flow exhaust model.

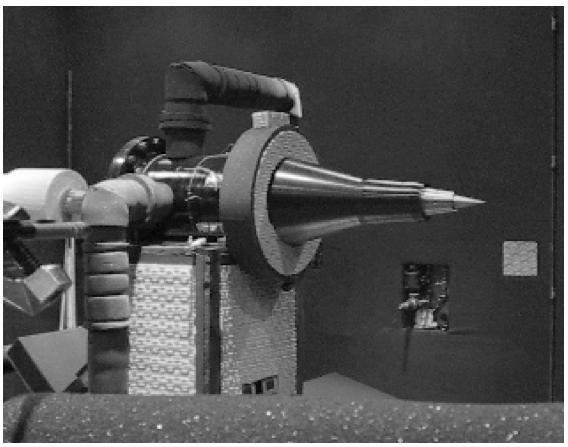

Fig. 2 UC coaxial acoustic test rig.

Table 1 Nozzle geometry summary

Nozzle	Number of chevrons	Penetration
Baseline	0	None
12LP	12	Nominal
8LP	8	Nominal
8HP	8	Increased

Table 2 Summary of test conditions

Test point	Core NPR	Core temp, K	Fan temp, K	$V_{\text{diff}}/V_{\text{mix}}$
1	1.85	395	288	1.12
2	1.85	395	288	0.87
3	1.85	395	288	0.58
4	1.85	395	288	0.27
5	1.85	395	288	0.11

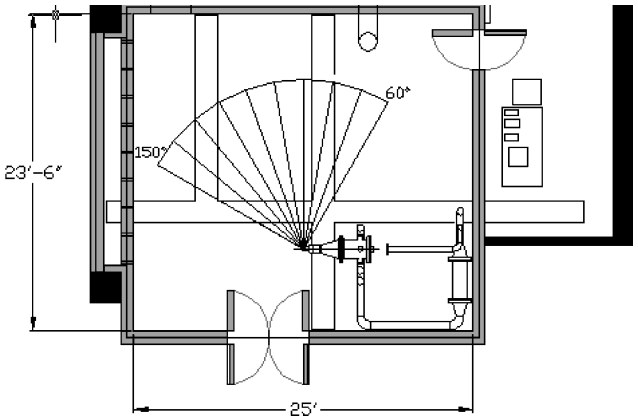

Fig. 3 Layout and dimensions of UC acoustic test facility.

Four different core nozzles were used in this study. This includes a baseline circular nozzle as well as three different chevron nozzles. The chevron nozzles were selected to provide insight into the effect of the number of chevrons as well as the level of penetration of the chevrons into the flow. One nozzle was a 12-lobe chevron with a nominal level of penetration. The other two nozzles each featured eight chevrons. One had the same nominal level of penetration as the 12-lobe nozzle, while the other had approximately twice this level of penetration. Figure 4 shows a photograph of the four nozzles used in the study, whereas the geometric details are summarized in Table 1.

Results and Discussion

The UC Nozzle Acoustic Test Rig was used to run a set of coaxial flow conditions, based on nozzle pressure ratio (NPR) and the velocity difference between the inner and outer flow streams. These test conditions are listed in Table 2. The normalized parameter $V_{\text{diff}}/V_{\text{mix}}$ was selected to define the operating condition, with V_{mix} being the mass averaged velocity of the two streams.

All of the data and results presented herein pertain to tests and measurements performed with scale-model nozzles and include only

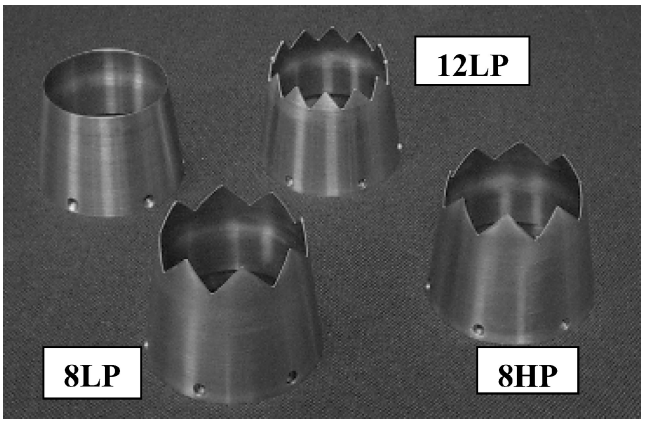

Fig. 4 Core nozzles used in study.

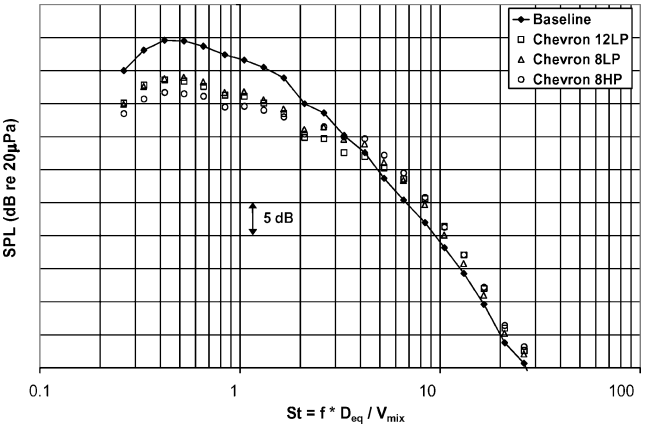

Fig. 5 Spectral comparison for V_{diff}/V_{mix}, 1.12; directivity angle, 150 deg.

jet noise measurements. All of the acoustic data have been scaled by a factor of 8, corresponding to the size of engines on current regional jet aircraft, extrapolated to a 1500-ft (457.2-m) sideline distance, and corrected to Society of Automotive Engineers 77 standard-day atmospheric conditions. In addition to this, the postprocessing code also computed standard noise metrics of perceived noise level (PNL) and EPNL. Although it is recognized that absolute EPNL computations are not defined for static jet noise measurements, by arbitrarily assigning a forward flight velocity to the static data, this parameter was calculated in order to allow comparisons between the various nozzles. As part of the EPNL calculation, the code also extrapolates and interpolates some additional angles required for the calculation. For OASPL and PNL directivity data presented here, note that angles in excess of 150 deg are extrapolated, whereas the 80-deg angle is interpolated. All other angles shown are measured angles.

Spectral Results

One-third octave-band spectral comparisons at directivity angles of 150 and 90 deg are shown for cycle points 1, 3, and 5 in Figs. 5–10. The 150-deg spectra were selected for presentation as this angle represents the nominal angle of peak jet noise emission, where the large, coherent turbulence structures are the dominant noise-generating mechansims.[11–13] In contrast, the 90-deg spectra were selected to show the impact of the various chevron nozzles at a forward directivity angle, where the fine-scale turbulence structures have been shown to be the dominant noise-generating mechanism.[11–15] At each of these operating points the chevron nozzles are seen to provide sound-pressure-level (SPL) reductions over some or all of the measured frequency range. Also, some definite trends with respect to nozzle operating point and geometry can be observed.

At the high normalized velocity difference of 1.12, Figs. 5 and 6 show that the chevron nozzles provide substantial low-frequency

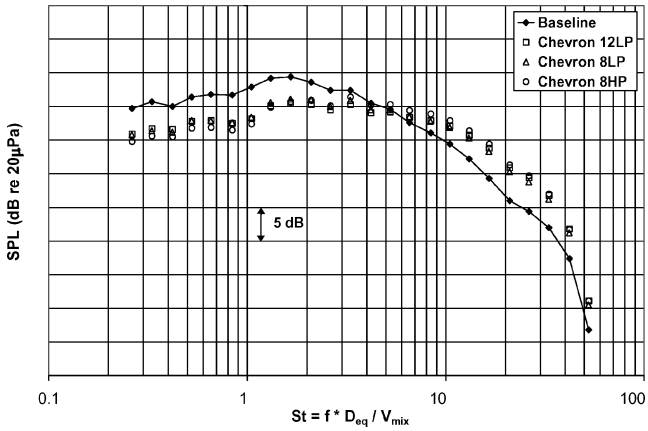

Fig. 6 Spectral comparison for V_{diff}/V_{mix}, 1.12; directivity angle, 90 deg.

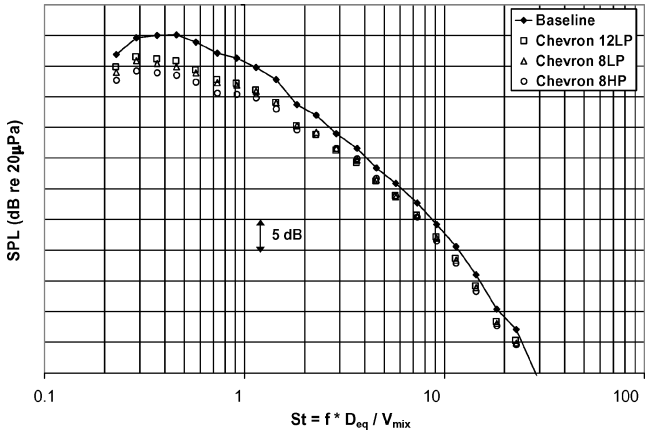

Fig. 7 Spectral comparison for V_{diff}/V_{mix}, 0.58; directivity angle, 150 deg.

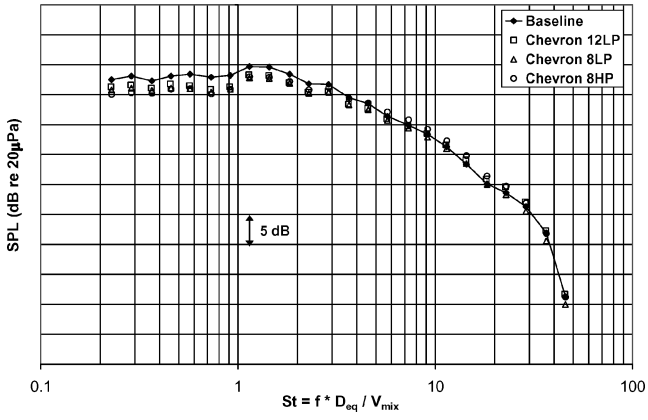

Fig. 8 Spectral comparison for V_{diff}/V_{mix}, 0.58; directivity angle, 90 deg.

SPL reduction at both directivity angles. For example, reductions as high as 8 dB are seen in the 150-deg spectrum at the lower frequencies. In the 90-deg spectra, the chevron nozzles provide low-frequency reductions ranging from 4 to 5 dB. Note that nozzle 8HP seems to provide the highest levels of SPL reduction at the low frequencies. In contrast to this low-frequency effectiveness, a crossover is seen at a mixed-velocity Strouhal number of approximately 3–4 at 150 deg and 4–5 at 90 deg. Above this point, each of the three chevron nozzles produces SPL increases. Of the three chevron nozzles, 8LP produces the least SPL increase, approximately 1–3 dB in the 150-deg spectrum and approximately 3–4 dB in the 90-deg spectra. By comparison, nozzles 12LP and 8HP each produce in

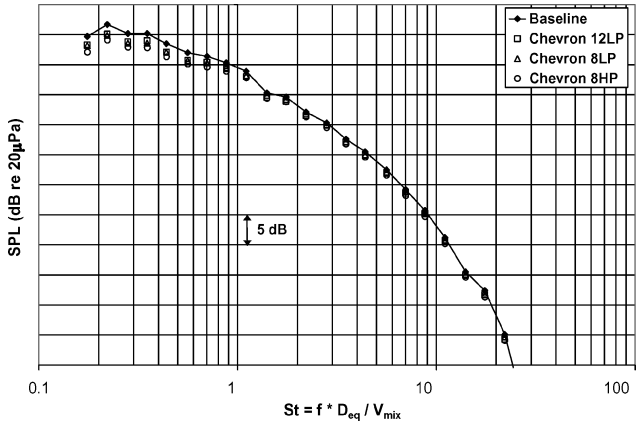

Fig. 9 Spectral comparison for V_{diff}/V_{mix}, 0.11; directivity angle, 150 deg.

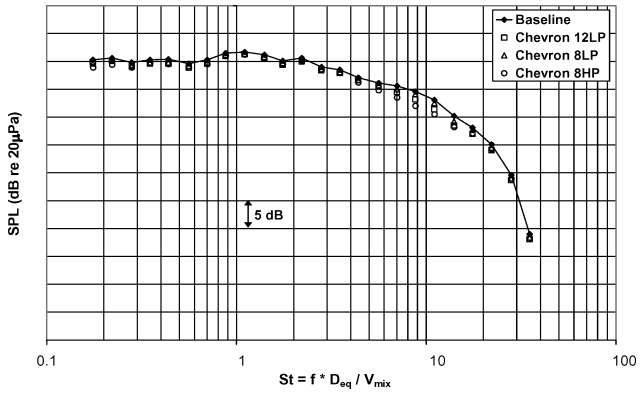

Fig. 10 Spectral comparison for V_{diff}/V_{mix}, 0.11; directivity angle, 90 deg.

excess of 3 dB high-frequency increase at the aft angles and 4–5 dB at 90 deg.

As the velocity difference is reduced to a normalized value of 0.58, the chevron benefit improves dramatically. Figures 7 and 8 show that the chevrons provide a more consistent level of SPL reduction at this more moderate velocity difference. At 150 deg, the low-frequency benefit is retained without the accompanying high-frequency increase seen in the higher-velocity difference case. Each of the three nozzles now provides SPL attenuation across the entire frequency range at the 150-deg directivity angle. However, the largest reductions are still seen at the lower frequencies. At Strouhal numbers below 2, SPL reductions ranging from 4 to 6.5 dB are given by the three nozzles with chevron 8HP again providing the greatest reduction. Above this Strouhal number, each of the three nozzles provides similar SPL benefit in the range of 2–3 dB. Similar results are seen in the 90-deg spectra, where nozzle 8LP provides the best SPL benefit with no crossover. Up to a Strouhal number of approximately 3.5, nozzle 8LP provides a 1–3-dB reduction. Above this point, it appears that this nozzle provides little attenuation. It is also notable that nozzles12LP and 8HP both produce a slight high-frequency crossover in the range of 1–2 dB. However, the extent of this increase is much less significant than the 4–5-dB increase that was seen for the higher-velocity difference of 1.12 at the same directivity angle.

Finally, as the nozzle velocity difference is reduced further, to a normalized value of 0.11, the chevron benefit at both directivity angles is dramatically diminished. The spectra at 150 deg for this cycle point are shown in Fig. 9. At this angle, it is readily apparent that any SPL reduction is very limited. Nozzle 8LP and 8HP do provide a 2–3-dB reduction, but this is restricted to Strouhal numbers less than 1. Above this frequency, none of the three chevron nozzles appears to have a significant effect on the baseline spectra. Note that the best low-frequency attenuation is again provided by nozzle

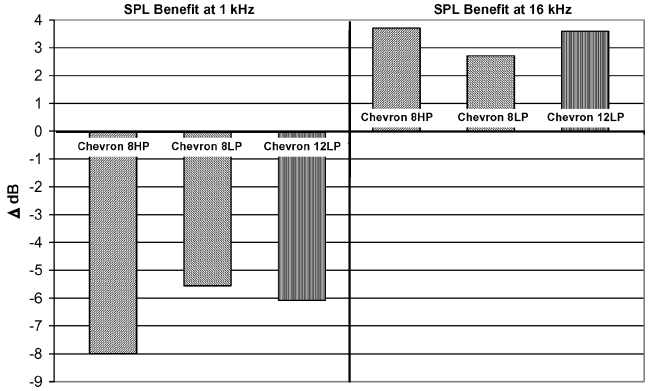

Fig. 11 Comparison of chevron SPL benefit at low- and high-frequency. Cycle condition 1; V_{diff}/V_{mix}, 1.12; directivity angle, 150 deg.

8HP. This is consistent with the observations made for the other two values of velocity difference. At 90 deg, it appears that each of the three chevrons produces less than 2 dB reduction at any frequency.

The spectral results presented in Figs. 5–10 indicate that the SPL effectiveness of the chevrons is strongly dependent on engine operating point with the velocity difference possibly being a critical parameter. Additionally, consistent differences in the spectral benefit provided by each of the three nozzles were observed. For example, the high penetration nozzle, 8HP, provided the greatest low-frequency benefit at all cycle conditions, while also consistently giving the least benefit at the high frequencies. In contrast, nozzle 8LP typically created more subtle changes to the baseline spectra with less low-frequency attenuation and less high-frequency amplification. This same tradeoff between low- and high-frequency benefit as a function of the chevron penetration was noted by Viswanathan in a recent publication.[16] The 12-lobe nozzle, 12LP, produced was typically shown to provide similar low-frequency benefit to that of nozzle 8LP, but the high-frequency effectiveness was closer to that of nozzle 8HP. Therefore, the increased lobe number appears to primarily affect the high-frequency effectiveness of the chevron. This contrast between and low- and high-frequency effectiveness is perhaps shown more illustratively in Fig. 11, which shows the aft-angle SPL benefit provided at cycle condition 1. This figure shows the SPL benefit at the peak baseline jet noise frequency of 1 kHz as well as the benefit provided at 16 kHz where the chevron gave the minimum benefit. The superior low-frequency benefit provided by the higher penetration nozzle is clear. At the low frequency, the benefit provided by the 12-lobe nozzle is similar to that provided by nozzle 8LP, which has the same penetration. At the high frequency, nozzle 8LP clearly produces the minimum SPL increase, with the high penetration producing the greatest SPL increase. The high-frequency effect of the number of chevrons is shown as well, as nozzle 12LP now produces a benefit more similar to that of 8HP than 8LP, indicating that the effect of chevron count becomes more important at higher frequencies.

The conclusions reached with regard to the effect of the chevron geometry agree with the prediction of an analytical model developed by Tam and Zaman for subsonic, single flow, tabbed jets.[17] This model effectively explains how tabbed nozzles generate high-frequency noise by shifting the peak jet noise to higher frequencies. The analytical expressions indicate that an increasing number of tabs (or chevrons) will produce a greater shift in peak frequency and thus generate additional high-frequency noise. This agrees with the preceding observation that the number of chevrons primarily affects the higher frequencies. Unfortunately, the model does not permit the effect of penetration to be explicitly evaluated. However, the model does indicate that the tabbed nozzles modify the flow structure to reduce the cross-sectional area of the primary jet and that the extent of high-frequency noise generation is proportional to this reduction in cross-sectional area. It is logical that increased chevron penetration will produce greater modification to the baseline jet structure than a lower penetration nozzle. Therefore, the observation that the

high penetration nozzle typically generates more high-frequency noise than the nominal penetration nozzles is consistent with the Tam model.

OASPL Directivity Results

Because of the spectral variation of the chevron benefit, especially the high-frequency crossover seen at the higher-velocity difference, it is necessary to consider integrated spectral metrics such as OASPL and PNL in order to quantify the relative acoustic benefits of the three chevron nozzles. Figures 12 and 13 show OASPL directivity plots for normalized velocity differences of 1.12 and 0.58, respectively. The OASPL is calculated over a narrowband bandwidth of 500 Hz–100 kHz. For these two nozzle operating conditions, the chevrons provide OASPL reductions at all directivity angles, despite the reduced high-frequency effectiveness seen in the spectra. This clearly shows that the substantial low-frequency benefit of the chevrons outweighs any high-frequency SPL increases to produce an overall noise reduction. However, it should be stressed that the same is not necessarily true of the PNL directivity, which applies frequency weighting to simulate the response of the human ear. It is also clear that the largest OASPL reductions are seen at the aft angles beyond 120 deg, with maximum reductions in excess of 7 dB at the most aft angle. The aft-angle effectiveness indicates that the chevrons are particularly effective at suppressing the noise generated by the large-scale coherent structures. As a result of this increased aft-angle benefit, the chevrons effectively produce a forward shift in the location of the peak OASPL. In these figures, the peak jet noise of the baseline nozzle occurs at a directivity angle of 150 deg. In contrast, the jet noise peaks at 130 deg for each of the chevron nozzles.

Figure 14 shows the OASPL directivity for the lowest normalized velocity difference of 0.11. Here, it is clearly apparent that the chevron benefit has been greatly diminished, with a maximum OASPL benefit of 2.3 dB given by nozzle 8HP. Note that this is approximately 60% less than the reduction provided by the same nozzle for the high-velocity difference case seen in Fig. 12. Furthermore, there is no apparent shift in the location of the peak jet noise for this case. As a result, the OASPL benefit does not show the same increase at the aft angles that was seen for the other two cycle conditions in Figs. 12 and 13.

The increased effectiveness at the aft directivity angles for the normalized velocity differences of 1.12 and 0.58 are emphasized by Figs. 15 and 16, which show the OASPL reduction for each of these cases. Although the chevron benefit is maximized at the aft angles as a result of the shift in the polar angle of the peak jet noise, it is not confined to this area. These figures show that forward of 120 deg, the chevron benefit is fairly constant with respect to angle and that there is little difference in the levels provided by the different nozzles. For the $V_{\text{diff}}/V_{\text{mix}}$ of 1.12, the reduction in this region is 2–3 dB, and it reduces slightly for the more moderate velocity difference case to 1–2 dB. At angles aft of 120 deg, the OASPL reduction

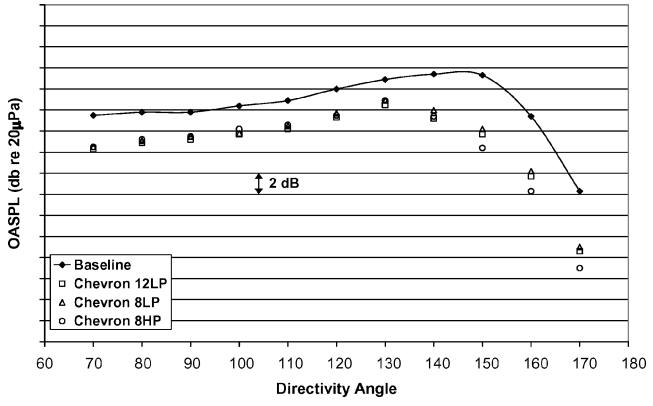

Fig. 12 OASPL directivity comparison for $V_{\text{diff}}/V_{\text{mix}}$: 1.12.

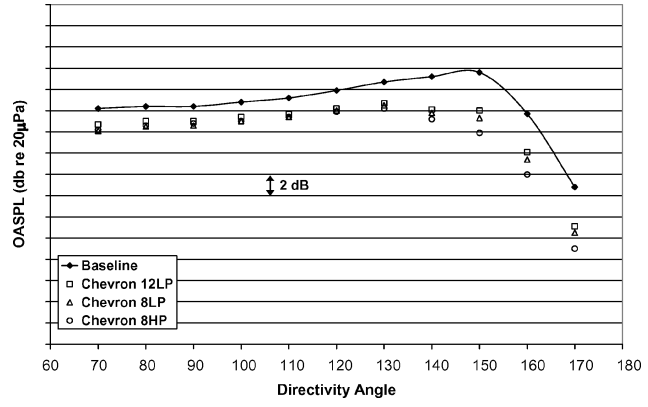

Fig. 13 OASPL directivity comparison for $V_{\text{diff}}/V_{\text{mix}}$: 0.58.

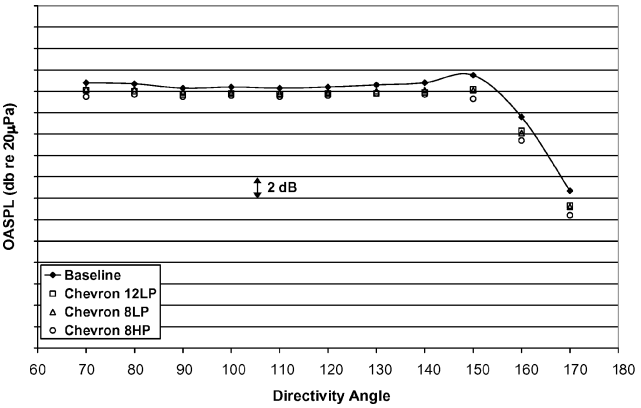

Fig. 14 OASPL directivity for $V_{\text{diff}}/V_{\text{mix}}$: 0.11.

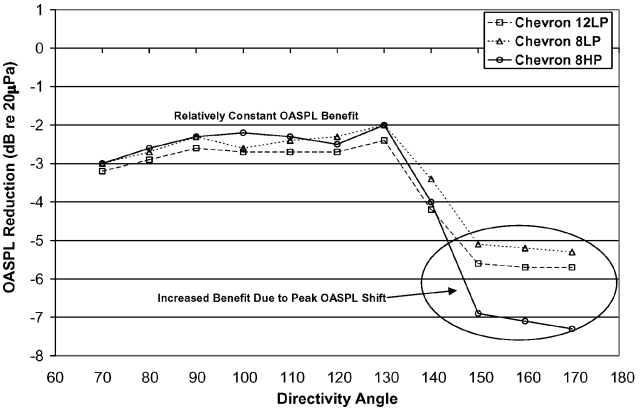

Fig. 15 OASPL reduction for $V_{\text{diff}}/V_{\text{mix}}$: 1.12.

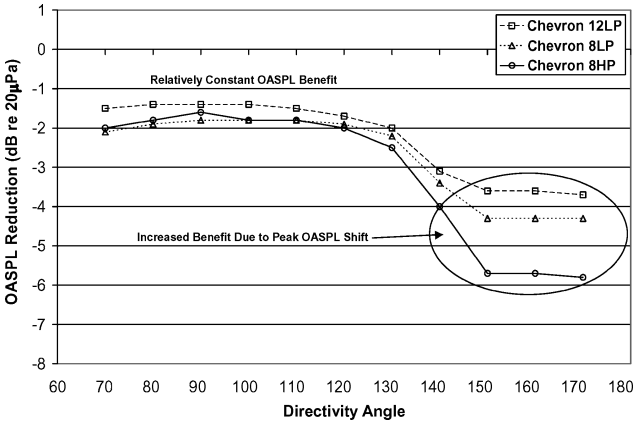

Fig. 16 OASPL reduction for $V_{\text{diff}}/V_{\text{mix}}$: 0.58.

is seen to increase by a factor of 2–3 for both operating conditions, with the higher penetration nozzle, 8HP, providing the greatest reductions.

The directivity results show consistency with the observations from the spectral plots and with previously documented jet noise characteristics. It has been well documented that jet noise exhibits preferential propagation with lower frequencies propagating mainly to the aft angles and higher frequencies being more efficient at upstream propagation.[11–15] Based on this accepted characteristic of jet noise, the increased aft-angle OASPL benefit is consistent with the spectra, which showed the chevrons to be most effective at lower frequencies. Likewise, the spectra showed the chevrons to be less effective at the higher frequencies, which is consistent with the reduced OASPL benefit at the more forward angles. This argument can be extended by considering the relative levels of reduction provided by the three chevron nozzles. The high penetration nozzle, 8HP, consistently provided the maximum low-frequency reduction in the spectra and was shown to provide maximum aft-angle OASPL reduction in Figs. 15 and 16.

The changes seen in the noise directivity, particularly the shift in the location of the peak jet noise, are a positive indication that the chevron nozzles are effectively modifying the jet plume and its associated noise-generating mechanisms. For example, it has been exhibited in tabbed nozzles that increased shear-layer mixing leads to a reduction in the jet potential core length.[3] This, in turn, can result in an accompanying shift in the location of the primary noise-generation zones. Furthermore, as the peak OASPL marks the outer edge of the "zone of silence" of the fine-scale noise generation, a forward shift in this peak represents an increase in the size of this zone. The existence of this region of reduced jet noise at aft angles is caused by mean flow refraction and was first observed experimentally in the 1960s by Atvars et al.[18] In the mid-1970s, Lilley modified the theoretical works of Lighthill and Ffowcs-Williams to account for this flow effect.[15] Additional discussion of the zone of silence has been provided more recently by Tam.[13] Today, this is an accepted characteristic of jet noise.

PNL Directivity Results

Although noise spectra and OASPL directivity plots can provide a great deal of insight into the raw physical effects of the various chevron nozzle parameters on the jet acoustics, weighted metrics such as PNL are required in order to assess the chevron potential from a noise certification stand point. Recall that PNL is an overall noise measure similar to OASPL except that frequency weighting is applied to simulate the response of the human ear. Therefore, although the low-frequency SPL reductions outweighed any high-frequency increases in the case of the OASPL directivity data the same is not necessarily true for PNL directivity. Also important is that the peak PNL contributes heavily to the EPNL, which is the standard metric used for aircraft noise certification.[19,20] Therefore, any reduction in peak PNL would likely result in a similar level of EPNL reduction. Figures 17 and 18 show plots of PNL directivity for normalized nozzle velocity differences of 1.12 and 0.58, respectively. The chevron effect is consistent with the OASPL directivity plots in that the maximum benefit is seen at the aft angles. In Fig. 17, nozzle 8LP provides PNL reductions at all directivity angles, including the peak level. In contrast, nozzles 12LP and 8HP both produce PNL increases at angles forward of 130 deg. This is not surprising based on the higher levels of high-frequency crossover produced by these two nozzles at this operating condition. Although these high-frequency increases did not lead to increases in OASPL, the weighting of the PNL calculation has enhanced the significance of the crossover. Perhaps more significantly, both of these nozzles are increasing the peak PNL, which implies that any EPNL reduction at this operating condition would probably be limited. However, the aft-angle PNL reductions are still more significant than any of the forward angle PNL increases so an EPNL reduction would be possible. At the more moderate normalized velocity difference of 0.58, the PNL benefit is improved for all three nozzles. Most notably, nozzles 12LP and 8HP are no longer producing PNL increases at the forward angles. At angles forward of 120 deg, the nozzles provide

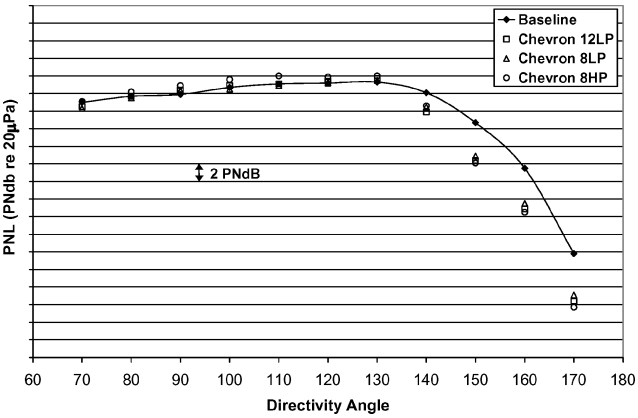

Fig. 17 PNL directivity for V_{diff}/V_{mix}: 1.12.

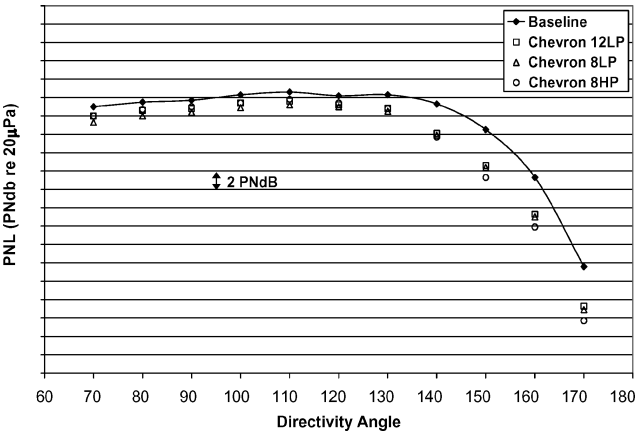

Fig. 18 PNL directivity for V_{diff}/V_{mix}: 0.58.

PNL reductions in the range of 1–2 PNdB with nozzle 8LP giving the largest reductions. At the aft angles, reductions of 4–6 PNdB are seen. In contrast to the higher-velocity difference case, each of the nozzles reduces the peak PNL by 1–2 PNdB, implying a potentially more significant EPNL benefit for this operating condition.

Chevron Effect on EPNL

A potential effect of the nozzle operating condition, specifically the velocity difference between the inner and outer flows, has been mentioned several times. Both the spectra and the directivity plots have provided clear indications that the acoustic benefit can be a function of this parameter. To investigate this dependence, a pseudo-EPNL was calculated from the static data using a forward flight Mach number of 0.3. Although it is recognized that the absolute value of such a pseudo-EPNL calculation cannot be considered meaningful, the difference in the values for the various nozzles can be. At the very least, such an analysis can give insight into any trends of the overall chevron acoustic benefit as a function of velocity difference. This EPNL calculation is based on measurements of jet noise only and does not account for any other component of engine noise. Figure 19 shows a plot of the EPNL reduction provided by the three chevron nozzles vs normalized nozzle velocity difference. This plot shows a consistent trend among the three nozzles and what seems to be a minimum at intermediate velocity differences. Finally, note that nozzle 8LP provides the maximum EPNL reduction of the three nozzles at −2.6 EPNdB. This should not come as a surprise based on Fig. 18, which showed that this nozzle provided the maximum reduction in peak PNL.

Additional data were also collected over a more extensive range of nozzle velocity differences for nozzle 8LP. These included cold flow data as well as the heated flow data shown in Fig. 19. Figure 20 shows the EPNL reduction provided by nozzle 8LP at each of the velocity differences tested. The error bars indicate ±0.3 EPNdB.

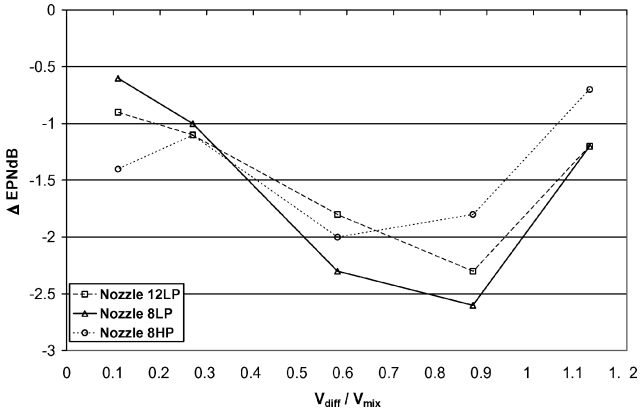

Fig. 19 EPNL reduction vs normalized velocity difference.

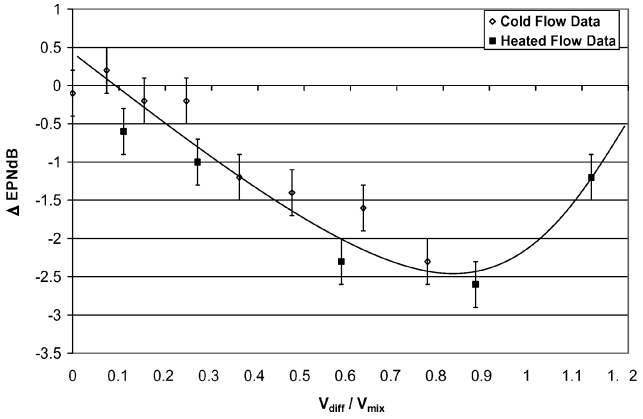

Fig. 20 EPNL reduction vs normalized velocity difference for nozzle 8LP.

This figure clearly shows an apparent minimum appearing in the same range of 0.8–0.9 as in Fig. 19 indicating that there does not seem to be a significant temperature effect for the range of temperatures tested. Figures 19 and 20 confirm that the acoustic benefit of a given chevron design is indeed a function of the velocity difference. As the velocity difference becomes higher, the increased shear-layer mixing as a result of the chevron becomes more aggressive, which can lead to high-frequency noise generation and a degradation or loss of the acoustic benefit. Conversely, as the velocity difference decreases, there might be insufficient shear to allow the chevrons to have a significant effect. In this way, the chevron nozzle becomes acoustically invisible with diminishing velocity difference. In Fig. 19 the two low penetration nozzles show a maximum EPNL reduction at normalized velocity difference of 0.8–0.9, whereas the higher penetration nozzle shows a maximum reduction at a lower-velocity difference of approximately 0.6. This shows a coupling effect between the chevron geometry and nozzle operating condition and implies that the chevron geometry, specifically the penetration, can be tailored to provide optimal reduction based on the design operating conditions of the exhaust system.

Single Flow Results

Finally, in addition to coaxial flow tests, single flow tests were conducted in order to verify the trends observed in the coaxial tests over a more extensive range of velocity differences. For these tests, nozzle pressure ratios ranging from 1.79 to 1.51 were tested in cold flow. It should be stressed that these single flow conditions will produce equivalent velocity differences well outside the intended design range of these chevron nozzles. Therefore, it was anticipated that the chevrons might not produce significant noise reduction under such flow conditions. Figures 21 and 22 show TOB spectra obtained for a cold flow nozzle pressure ratio of 1.68 at directivity angles of 150 and 90 deg, respectively. Analysis of these spectra indicates similar

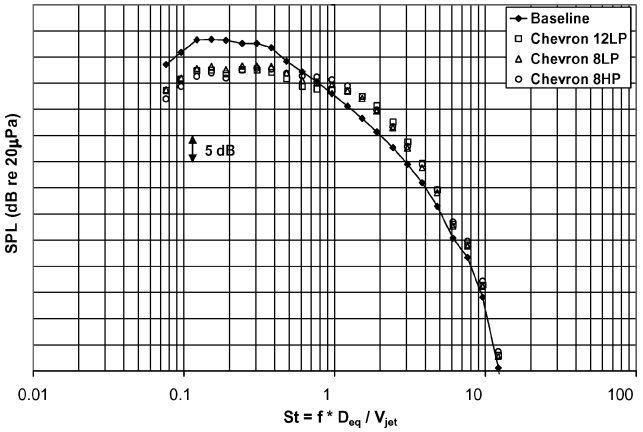

Fig. 21 Single flow spectral comparison: NPR, 1.68; T_0, 80°F; directivity angle, 150 deg.

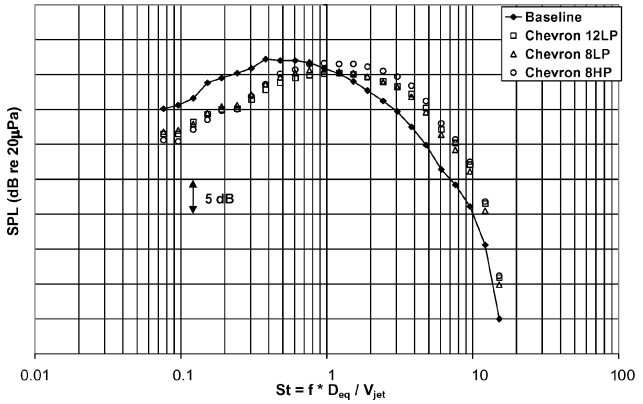

Fig. 22 Single flow spectral comparison: NPR, 1.68; T_0, 80°F; directivity angle, 90 deg.

effects for each of the three chevron nozzles in that a SPL reduction is observed at low frequencies with an accompanying increase at high frequencies. This is consistent with the trends observed in Figs. 5 and 6 for the coaxial flow at the highest velocity difference. However, it should be immediately evident that the high-frequency increase is much more severe in these single flow spectra. As the equivalent velocity difference of the nozzle would be substantially higher than that tested in any of the dual flow cycle points, this provides additional evidence that the velocity difference likely correlates directly with the observed high-frequency SPL increases for a given chevron design. The crossover in the single flow case is seen to occur at a model scale Strouhal number of approximately 0.8–0.9 for all of the nozzles. However, the extent of the reduction and crossover varies for the three nozzles. The greatest SPL reduction occurs at the aft angle with a reduction of 7 dB being provided by nozzle 8HP at a Strouhal number of 0.19. In the 90-deg spectra, each nozzle provides reductions in the range of 4–5 dB. It is also evident that nozzles 12LP and 8HP produce the greatest degree of high-frequency crossover with SPL increases of up to 4–5 dB at both directivity angles. By contrast, nozzle 8LP provides 5.6 dB of aft-angle reduction at the same Strouhal number of 0.19, but produces approximately 20–30% less high-frequency increase than nozzle 8HP at both directivity angles. Similar results were seen for all of the nozzle pressure ratios used in the single flow tests. The relative benefit of the three nozzles as well as the trends with frequency and directivity are all consistent with those observed for the dual flow cases. As the high-frequency crossover is obviously more extreme in these single flow cases, with higher effective velocity differences, these data provide additional evidence that the crossover is likely related to excessively high-velocity difference for the given chevron designs.

Measurement of the PNL directivity for cold flow nozzle pressure ratios of 1.79 and 1.51 is presented in Figs. 23 and 24. At these

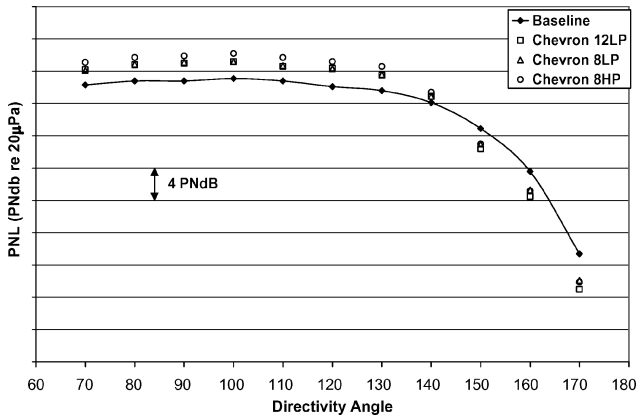

Fig. 23 Single flow PNL directivity comparison: NPR, 1.79; T_0, 80°F.

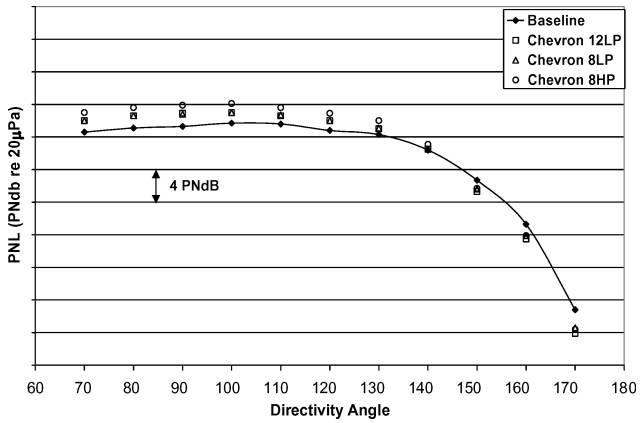

Fig. 24 Single flow PNL directivity comparison: NPR, 1.51; T_0, 80°F.

single flow operating conditions each of the three nozzles produces PNL increases at all angles forward of 150 deg. Comparison of these PNL directivities with those shown in Figs. 17 and 18 for the dual flow cases clearly shows that the forward angle PNL increase is much more severe (up to 3 PNdB increase) than any seen in the dual flow cases. This is consistent with the more severe high-frequency crossover seen in the single flow spectra. Other consistencies with the spectra can be seen as well. For example, note that the high penetration nozzle, 8HP, produces the largest amounts of high-frequency noise in Figs. 21 and 22. Therefore, it is not surprising to see that this nozzle also generates the largest PNL increases at the forward angles. The forward angle PNL increase becomes less severe as the nozzle pressure ratio is reduced from 1.79 to 1.51 producing a corresponding reduction in the effective velocity difference. These observations are all consistent with the conclusion that the velocity difference and the chevron penetration have a direct impact on the chevron benefit.

Summary

Spectral and overall sound pressure level (OASPL) directivity results showed the chevron nozzles were most effective at lower frequencies and at aft angles. These results are consistent with the well-documented directional characteristics of jet noise. OASPL directivity data showed that the increased aft-angle benefit of the chevrons produced an effective shift in the location of the peak jet noise. This shift in peak OASPL indicates that the chevrons are modifying the jet exhaust plume in a manner to decrease the size and/or location of the primary noise-generation region, likely shortening the potential core.

Additionally, clear and consistent trends in the acoustic benefit with respect to various chevron geometric parameters were documented. Effects directly attributable to the chevron penetration and number of lobes were observed. In all cases, the higher penetration nozzle, 8HP, was seen to produce the most significant modification of the baseline spectra. Depending on the operating condition and directivity angle, this nozzle was shown to produce low-frequency SPL reductions up to 8 dB for dual flow. However, this nozzle was also shown to be the least effective at high frequencies, with SPL increases of up to 4–5 dB. In contrast, the lower penetration nozzles, 8LP and 12LP, were shown to produce more subtle modifications to the baseline spectra. As a result, the high-frequency acoustic benefit of these nozzles was superior to that of nozzle 8HP. Similar trends of high-frequency crossover have been observed by researchers using tabbed nozzles, which are known to increase shear-layer mixing much more aggressively than do chevron nozzles.[3,9] Therefore, these results imply that the chevron penetration level directly influences the shear-layer mixing, and perhaps the higher penetration of nozzle 8HP has generated overly aggressive mixing, which is leading to the high-frequency noise generation.

In addition to the effect of the chevron geometric parameters, the data also illustrated that the benefit provided by a particular chevron configuration are strongly dependent on the velocity difference between the inner and outer flow streams. The coaxial and single flow spectra have clearly shown that the high-frequency sound pressure level (SPL) increase becomes more severe as the velocity difference increases. The dependence of the chevron EPNL benefit on the velocity difference was illustrated by Figs. 19 and 20. These figures indicate that the chevron acoustic benefit is maximized at intermediate values of velocity difference. As the velocity difference increases, it is likely that the mixing becomes overly aggressive, which leads to the high-frequency increase seen in the spectra in Figs. 5 and 6. This trend was verified by the more severe high-frequency SPL increase seen in the single flow data, which would be characteristic of even higher-velocity differences. Obviously, the loss of acoustic benefit at low-velocity differences should be expected. As chevron nozzles are designed to increase the efficiency of shear-layer mixing, it is reasonable that their ability to do this diminishes as the shear layer becomes weaker. The existence of this optimal range of velocity difference, as well as the evidence that the exact value of the optimal difference likely varies as the chevron penetration varies, emphasizes that the chevron design is quite application specific.

In conclusion, this work illustrates both the acoustic benefits that can be provided by well-designed chevron nozzles, as well as the sensitivity of these benefits to various chevron geometric parameters and nozzle operating condition. From the data presented, it should be relatively clear that these parameters likely exhibit coupling effects and cannot be optimized in an isolated manner. Obviously, care should be taken to use these nozzles at or near the design point in order to obtain maximum acoustic benefit. Likewise, for a fixed operating point both the level of penetration, as well as the number of chevron lobes, was shown to influence the acoustic benefit. It was shown that the penetration level can be carefully selected in order to balance the low-frequency SPL reduction with any potential high-frequency SPL increase and therefore tailor the desired impact on noise metric such as the effective perceived noise level. Furthermore, these chevron parameters must be optimized while taking into account the complete impact to the engine system, including performance, operability, manufacturing, structural integrity, and engine life. Future tests will be dedicated to extensive flowfield analysis using hot-film anemometry and particle imaging velocimetry. The results of the tests will be used to validate the conclusions that were reached in this study.

Acknowledgments

We acknowledge General Electric Aircraft Engines of Cincinnati, Ohio, for providing funding and technical assistance with this research study. Specifically, we thank Mike Benzakein, Dave Wisler, Richard Cedar, Kevin Early, and Phil Gliebe of General Electric Aircraft Engines.

References

[1] Bradbury, L. J. S., and Khadem, A. H., "The Distortion of a Jet by Tabs," *Journal of Fluid Mechanics*, Vol. 70, Pt. 4, 1975, pp. 801–813.

[2]Ahuja, K. K., and Brown, W. H., "Shear Flow Control by Mechanical Tabs," AIAA Paper 89-0994, March 1989.

[3]Samimy, M., Zaman, K. B. M. Q., and Reeder, M. F., "Effect of Tabs on the Flow and Noise Field of an Axisymmetric Jet," *AIAA Journal*, Vol. 31, No. 4, 1993, pp. 609–619.

[4]Ahuja, K. K., Manes, J. P., and Massey, K. C., "An Evaluation of Various Concepts of Reducing Supersonic Jet Noise," AIAA Paper 90-3982, Oct. 1990.

[5]Saiyed, N. H., and Bridges, J. E., "Tabs and Mixers for Reducing Low Bypass Ratio Jet Noise," AIAA Paper 99-1986, May 1999.

[6]Krothapalli, A., and King, C. J., "The Role of Streamwise Vortices on Sound Generation of a Supersonic Jet," AIAA Paper 93-4320, Oct. 1993.

[7]Salikuddin, M., Martens, S., Janardan, B. A., Shin, H., and Majjigi, R. K., "Experimental Study for Mult-Lobed Mixer High Bypass Exhaust Systems for Subsonic Jet Noise Reduction—Part 2: Acoustic Results," AIAA Paper 99-1988, May 1999.

[8]Gliebe, P. R., Brausch, J. F., Majjigi, R. K., and Lee, R., "Jet Noise Suppression," *Aeroacoustics of Flight Vehicles Vol 2. Noise Suppression*, edited by H. H. Hubbard, Acoustical Society of America, Woodbury, NY, 1995, pp. 207–269.

[9]Saiyed, N. H., Mikkelsen, K. L., and Bridges, J. E., "Acoustics and Thrust of Separate-Flow Exhaust Nozzles with Mixing Devices for High-Bypass-Ratio Engines," AIAA Paper 2000-1961, June 2000.

[10]Callender, B., Gutmark, E., and DiMicco, R., "Design and Validation of a Coaxial Nozzle Acoustic Test Facility," AIAA Paper 2002-0369, Jan. 2002.

[11]Tam, C. K. W., "Supersonic Jet Noise," *Annual Review of Fluid Mechanics*, Vol. 27, 1995, pp. 17–43.

[12]Tam, C. K. W., Golebiowski, M., and Siener, J. M., "On the Two Components of Turbulent Mixing Noise from Supersonic Jets," AIAA Paper 96-1716, May 1996.

[13]Tam, C. K. W., "Jet Noise Since 1952," *Theoretical and Computational Fluid Dynamics*, Vol. 10, 1998, pp. 393–405.

[14]Ffowcs-Williams, J. E., "The Noise of Turbulence Convected at High Speed," *Philosophical Transactions of the Royal Society of London, Ser. A*, Vol. 255, No. 1061, 1963, pp. 469–503.

[15]Lilley, G. M., "On the Noise from Jets. Noise Mechanisms," AGARD CP-131, 1974, pp. 13.1, 13.2.

[16]Viswanathan, K., "Jet Aeroacoustic Testing: Issues and Implications," *AIAA Journal*, Vol. 41, No. 9, 2003, pp. 1674–1689.

[17]Tam, C. K. W., and Zaman, K. B. M. Q., "Subsonic Jet Noise from Nonaxisymmetric and Tabbed Nozzles," *AIAA Journal*, Vol. 38, No. 4, 2000, pp. 592–599.

[18]Atvars, J., Schubert, L. K., and Ribner, H. S., "Refraction of Sound from a Point Source Located in an Air Jet," *Journal of Acoustical Society of America*, Vol. 37, 1965, pp. 168–170.

[19]Powell, C. A., and Fields, J. M., "Human Response to Aircraft Noise," *Aeroacoustics of Flight Vehicles*, edited by H. H. Hubbard, Vol. 2, Acoustical Society of America, Woodbury, NY, 1995, pp. 1–52.

[20]Peart, N. A., "Fly-Over Noise Measurement and Prediction," *Aeroacoustics of Flight Vehicles*, edited by H. H. Hubbard, Vol. 2, Acoustical Society of America, Woodbury, NY, 1995, pp. 357–382.

W. Ng
Associate Editor